J Physiol 588.23 (2010) pp 4743–4757

The Journal of Physiology

Ca^{2+} spark-dependent and -independent sarcoplasmic reticulum Ca^{2+} leak in normal and failing rabbit ventricular myocytes

Aleksey V. Zima[1], Elisa Bovo[1], Donald M. Bers[2] and Lothar A. Blatter[3]

[1]*Department of Cell and Molecular Physiology, Loyola University Chicago, Stritch School of Medicine, 2160 South First Avenue, Maywood, IL 60153, USA*
[2]*Department of Pharmacology, University of California Davis, Genome Building 3511, Davis, CA 95616, USA*
[3]*Department of Molecular Biophysics and Physiology, Rush University Medical Center, 1750 West Harrison Street, Chicago, IL 60612, USA*

Sarcoplasmic reticulum (SR) Ca^{2+} leak is an important component of cardiac Ca^{2+} signalling. Together with the SR Ca^{2+}-ATPase (SERCA)-mediated Ca^{2+} uptake, diastolic Ca^{2+} leak determines SR Ca^{2+} load and, therefore, the amplitude of Ca^{2+} transients that initiate contraction. Spontaneous Ca^{2+} sparks are thought to play a major role in SR Ca^{2+} leak. In this study, we determined the quantitative contribution of sparks to SR Ca^{2+} leak and tested the hypothesis that non-spark mediated Ca^{2+} release also contributes to SR Ca^{2+} leak. We simultaneously measured spark properties and intra-SR free Ca^{2+} ($[Ca^{2+}]_{SR}$) after complete inhibition of SERCA with thapsigargin in permeabilized rabbit ventricular myocytes. When $[Ca^{2+}]_{SR}$ declined to $279 \pm 10\ \mu M$, spark activity ceased completely; however SR Ca^{2+} leak continued, albeit at a slower rate. Analysis of sparks and $[Ca^{2+}]_{SR}$ revealed, that SR Ca^{2+} leak increased as a function of $[Ca^{2+}]_{SR}$, with a particularly steep increase at higher $[Ca^{2+}]_{SR}$ ($>600\ \mu M$) where sparks become a major pathway of SR Ca^{2+} leak. At low $[Ca^{2+}]_{SR}$ ($<300\ \mu M$), however, Ca^{2+} leak occurred mostly as non-spark-mediated leak. Sensitization of ryanodine receptors (RyRs) with low doses of caffeine increased spark frequency and SR Ca^{2+} leak. Complete inhibition of RyR abolished sparks and significantly decreased SR Ca^{2+} leak, but did not prevent it entirely, suggesting the existence of RyR-independent Ca^{2+} leak. Finally, we found that RyR-mediated Ca^{2+} leak was enhanced in myocytes from failing rabbit hearts. These results show that RyRs are the main, but not sole contributor to SR Ca^{2+} leak. RyR-mediated leak occurs in part as Ca^{2+} sparks, but there is clearly RyR-mediated but Ca^{2+} sparks independent leak.

(Received 12 August 2010; accepted after revision 13 October 2010; first published online 20 October 2010)
Corresponding author A. V. Zima: Department of Cell and Molecular Physiology, Loyola University Chicago, Stritch School of Medicine, 2160 South First Avenue, Maywood, IL 60153, USA. Email: azima@lumc.edu

Abbreviations 2-APB, 2-aminoethoxydiphenyl borate; $[Ca^{2+}]_i$, cytosolic free calcium concentration; $[Ca^{2+}]_{SR}$, sarcoplasmic reticulum free calcium concentration; ECC, excitation–contraction coupling; HF, heart failure; IP_3R, inositol-1,4,5-trisphosphate receptor; NCX, Na^+–Ca^{2+} exchanger; PLB, phospholamban; RuR, ruthenium red; RyR, ryanodine receptor; SERCA, sarcoplasmic/endoplasmic reticulum Ca^{2+}-ATPase; SR, sarcoplasmic reticulum; TG, thapsigargin.

Introduction

During cardiac excitation–contraction coupling (ECC), simultaneous activation of sarcoplasmic reticulum (SR) ryanodine receptor (RyR; type 2) Ca^{2+} release channels generates global Ca^{2+} transients required for activation of contraction. After termination of SR Ca^{2+} release, a significant portion of cytosolic Ca^{2+} is sequestered back into the SR by the Ca^{2+}-ATPase (SERCA) leading to cardiac muscle relaxation. During diastole, RyRs are not completely quiescent, thus providing a pathway for significant SR Ca^{2+} leak. Therefore, the finite balance between SR Ca^{2+} uptake and leak determines the amount of Ca^{2+} stored in the SR. Because the fractional SR Ca^{2+} release steeply depends on SR Ca^{2+} load (Bassani *et al.* 1995), a small shift in this balance can lead to substantial changes in SR Ca^{2+} load and, therefore, Ca^{2+} transient amplitude. While it is well established that SR Ca^{2+} uptake

DOI: 10.1113/jphysiol.2010.197913

is entirely mediated by SERCA pump activity, the specific pathways of SR Ca^{2+} leak have not been characterized in detail.

In ventricular myocytes SR Ca^{2+} release during ECC occurs at specialized release sites where L-type Ca^{2+} channels in the T-tubules are closely associated with the RyR clusters of the junctional SR. The release cluster contains dozens of, possibly more than 100, RyRs (Franzini-Armstrong & Protasi, 1997) and their simultaneous activation produces the elementary release events termed Ca^{2+} sparks (Cheng *et al.* 1993). During ECC, the global Ca^{2+} transient is the result of spatio-temporal summation of Ca^{2+} release from thousands of these individual release sites. Ca^{2+} sparks can also occur spontaneously during rest or diastole providing an important pathway for SR Ca^{2+} leak. It has been proposed that Ca^{2+} release in the form of sparks can explain almost the entire diastolic SR Ca^{2+} leak (Cheng *et al.* 1993; Bassani & Bers, 1995). However, a growing body of evidence suggests that SR Ca^{2+} leak may also occur as undetectable openings of RyRs (non-spark RyR-mediated SR Ca^{2+} leak). In ventricular myocytes, Ca^{2+} sparks are rare events during diastole suggesting that SR Ca^{2+} release events with amplitudes that are significantly smaller than typical sparks are responsible for a major part of SR Ca^{2+} leak (Santiago *et al.* 2010). Potential mechanisms include spontaneous openings of single RyR in a release cluster without activation of the remaining channels in the cluster (Lipp & Niggli, 1996), activation of isolated unclustered RyRs (Sobie *et al.* 2006), or non-RyR leak pathways. However, it remains elusive to what degree these different types of Ca^{2+} release events contribute to the global SR Ca^{2+} leak and how these release events are dependent on SR Ca^{2+} load.

Heart failure (HF) is commonly associated with decreased contractile function due to alterations of the activity of several important Ca^{2+} transport systems, including the RyR. Increased RyR-mediated Ca^{2+} leak during HF has been implicated in reduction of SR Ca^{2+} content and triggering of Ca^{2+}-dependent arrhythmias (George, 2008). Abnormal phosphorylation of RyR by either protein kinase A (Marx *et al.* 2000) or Ca^{2+}–calmodulin-dependent kinase II (Ai *et al.* 2005) has been shown to contribute to enhanced SR Ca^{2+} leak in HF. Furthermore, redox modification of the RyR also plays a functional role in changes of SR Ca^{2+} leak in failing hearts (Terentyev *et al.* 2008). In addition, contributions from non-RyR Ca^{2+} leak need to be considered. A prime candidate in this context is the inositol-1,4,5-trisphosphate receptor (IP_3R) SR Ca^{2+} release channel. Although expressed at lower densities compared to RyRs, IP_3R-dependent Ca^{2+} release modulates ECC and contributes to arrhythmogenesis (Proven *et al.* 2006; Domeier *et al.* 2008). IP_3Rs are upregulated during HF (Go *et al.* 1995; Ai *et al.* 2005) and thus may contribute to the enhanced SR Ca^{2+} leak. Therefore, it is critically important to characterize the mechanisms of SR Ca^{2+} leak for better understanding of cardiac Ca^{2+} signalling under normal conditions and in disease states.

In this study, we investigated mechanisms of SR Ca^{2+} leak in rabbit ventricular myocytes, with a particular interest in the role of Ca^{2+} sparks. Spontaneous Ca^{2+} sparks have been used extensively as the index of SR Ca^{2+} leak in cardiomyocytes. Although previous studies provide important information about RyR regulation and Ca^{2+} signalling, it remains unclear whether or not Ca^{2+} sparks are the major pathway of SR Ca^{2+} leak. Here, we employed a newly developed approach to directly measure SR Ca^{2+} leak as changes of $[Ca^{2+}]_{SR}$ after complete SERCA inhibition. To measure $[Ca^{2+}]_{SR}$ we used the low affinity Ca^{2+} indicator Fluo-5N entrapped within the SR. After permeabilization of the sarcolemma, the high affinity Ca^{2+} indicator Rhod-2 was added to the cytosol to measure Ca^{2+} sparks simultaneously. This experimental approach allowed us to directly and continuously study the functional relationship between Ca^{2+} spark properties and SR Ca^{2+} leak. We found that in rabbit ventricular myocytes RyRs were the main pathway for SR Ca^{2+} leak which occurred in the form of Ca^{2+} sparks, but also as spark-independent Ca^{2+} leak. At low $[Ca^{2+}]_{SR}$, leak occurred mostly in the absence of sparks, whereas at high $[Ca^{2+}]_{SR}$, Ca^{2+} sparks became a significant contributor to SR Ca^{2+} leak. The spark-independent Ca^{2+} leak consisted of at least two components: undetectable Ca^{2+} release through RyRs and Ca^{2+} efflux through pathways other than RyRs and IP_3Rs; however stimulation with IP_3 increased RyR-independent leak. We also found that SR Ca^{2+} leak was significantly increased in ventricular myocytes from failing hearts. This effect was attributed to an increased RyR activity. Part of this work has been published in abstract form (Zima & Blatter, 2009).

Methods

Myocyte isolation

Ventricular myocytes were isolated from New Zealand White rabbits (30 animals, 2.5 kg; Myrtle's Rabbitry, Thompsons Station, TN, USA) or rabbits with non-ischaemic HF induced by combined aortic insufficiency and stenosis (5 animals, for detailed description of HF model see Pogwizd, 1995). The procedure of cell isolation was approved by the Institutional Animal Care and Use Committee, and complies with US and UK regulations on animal experimentation (Drummond, 2009). Adult rabbits were anaesthetized with sodium pentobarbital (50 mg kg^{-1} I.V.). Following thoracotomy hearts were quickly excised, mounted on a Langendorff apparatus, and retrogradely

perfused with collagenase-containing solution at 37°C according to the procedure described previously (Domeier *et al.* 2009). All chemicals and reagents were purchased from Sigma-Aldrich (St Louis, MO, USA).

Confocal microscopy

For simultaneous recording of $[Ca^{2+}]_{SR}$ and $[Ca^{2+}]_i$ we used the low affinity Ca^{2+} indicator Fluo-5N and the high affinity Ca^{2+} indicator Rhod-2, respectively (indicators obtained from Molecular Probes/Invitrogen, Carlsbad, CA, USA). Myocytes were incubated with 5 μM of Fluo-5N/AM for 2.5 hours at 37°C as described before (Zima *et al.* 2008*b*; Domeier *et al.* 2009). Fluo-5N/AM loaded myocytes were permeabilized with saponin (Zima *et al.* 2008*a*) to remove cytosolic Fluo-5N. The saponin free internal solution was composed of (in mM): potassium aspartate 100; KCl 15; KH_2PO_4 5; MgATP 5; EGTA 0.35; $CaCl_2$ 0.12; $MgCl_2$ 0.75; phosphocreatine 10; Hepes 10; Rhod-2 tripotassium salt 0.04; creatine phosphokinase 5 U ml^{-1}; dextran (MW: 40,000) 8%; pH 7.2 (KOH). Free $[Ca^{2+}]$ and $[Mg^{2+}]$ of this solution were 150 nM and 1 mM, respectively. All experiments were performed at room temperature (20–24°C).

Changes in $[Ca^{2+}]_i$ and $[Ca^{2+}]_{SR}$ were measured with laser scanning confocal microscopy (Radiance 2000 MP, Bio-Rad, UK) equipped with a ×40 oil-immersion objective lens (NA = 1.3). Fluo-5N was excited with the 488 nm line of an argon ion laser and fluorescence was measured at 515 ± 15 nm. Rhod-2 was excited with the 543 nm line of a He–Ne laser and fluorescence was measured at wavelengths >600 nm. Images were acquired in line-scan mode (3 ms per scan; pixel size 0.12 μm). The axial resolution was 1.1 μm at full-width half-maximum (point-spread function determined experimentally).

Measurements of Ca^{2+} sparks

Ca^{2+} sparks were detected and analysed using SparkMaster (Picht *et al.* 2007). To exclude false positive events, a threshold criterion for spark detection of 3.8 was chosen. At this threshold no events were detected when SR Ca^{2+} was emptied after simultaneous application of caffeine (10 mM) and thapsigargin (TG; 10 μM). Analysis of Ca^{2+} sparks included frequency (sparks (100 μm)$^{-1}$ s^{-1}), amplitude ($\Delta F/F_0$), full duration at half-maximal amplitude (FDHM; ms), and full width at half-maximal amplitude (FWHM; μm). F_0 is the initial fluorescence recorded under steady-state conditions and $\Delta F = F - F_0$. Spark frequency was corrected for missing events as described previously (Song *et al.* 1997; see online Supplemental Material). Ca^{2+} release flux (Sipido & Wier, 1991) and signal mass (Chandler *et al.* 2003) were used to estimate releasable Ca^{2+} during individual spark. The SR Ca^{2+} release flux was estimated from the peak of the first derivative of the cytosolic fluorescence intensity and expressed as $d(\Delta F/F_0)/dt$ (ms^{-1}). Signal mass of Ca^{2+} sparks was calculated according to the formula: $SM_{spark} = 1.206 \times \Delta F/F_0 \times FWHM^3$. By measuring Ca^{2+} sparks in control and Fluo-5N-loaded cells, we also found that loading of the SR with Fluo-5N did not significantly affect spark properties and SR Ca^{2+} load (see online Supplemental Material).

Measurements of SR Ca^{2+} leak

To minimize indicator photobleaching, Fluo-5N was excited with minimum laser energy. To improve the signal-to-noise ratio of the low intensity Fluo-5N signal, fluorescence was collected with an open pinhole (non-confocal settings) and averaged over the entire cellular width of line-scan image (Figs 1*A* and 4*A*). At the end of each experiment minimum (F_{min}) and maximum (F_{max}) Fluo-5N fluorescence were estimated. F_{min} was measured after depletion of the SR with 10 mM caffeine in the presence of 5 mM EGTA ($[Ca^{2+}]$ ~5 nM). F_{max} was measured following an increase of $[Ca^{2+}]$ to 10 mM. Caffeine (10 mM) keeps RyRs open allowing $[Ca^{2+}]$ equilibration across the SR membrane (Shannon *et al.* 2003*a*). To prevent irreversible cell contraction during application of high $[Ca^{2+}]$, cells were pretreated for 5 min with the muscle contraction uncouplers 2,3-butanedione monoxime (10 mM) and blebbistatin (10 μM). Caffeine (10 mM) decreased Fluo-5N fluorescence by 16% due to chemical quenching of the dye. Therefore, F_{max} and F_{min} values were corrected accordingly. After correction, the Fluo-5N signal was converted to $[Ca^{2+}]$ using the formula: $[Ca^{2+}]_{SR} = K_d \times (F - F_{min})/(F_{max} - F)$, where K_d (Ca^{2+} dissociation constant) was 390 ± 35 μM ($n = 5$ cells) based on *in vivo* calibrations (see Supplemental Material). SR Ca^{2+} leak was measured as the changes of total $[Ca^{2+}]_{SR}$ ($[Ca^{2+}]_{SRT}$) over time ($d[Ca^{2+}]_{SRT}/dt$) after complete SERCA inhibition with TG. $[Ca^{2+}]_{SRT}$ was calculated as: $[Ca^{2+}]_{SRT} = B_{max}/(1 + K_d/[Ca^{2+}]_{SR}) + [Ca^{2+}]_{SR}$; where B_{max} and K_d were 2700 μM and 630 μM, respectively (Shannon *et al.* 2000*b*). The rate of SR Ca^{2+} leak ($d[Ca^{2+}]_{SRT}/dt$) was plotted as a function of $[Ca^{2+}]_{SR}$ for each time point (30 s) during $[Ca^{2+}]_{SR}$ decline. The complete SERCA inhibition was confirmed by measuring $[Ca^{2+}]_{SR}$ recovery after SR Ca^{2+} depletion with caffeine and then $[Ca^{2+}]_i$ elevation to drive Ca^{2+} uptake. TG (10 μM) completely prevented $[Ca^{2+}]_{SR}$ recovery within 1 min (data not shown). Based on Fluo-5N sensitivity to Ca^{2+}, it seems unlikely that Fluo-5N trapped in mitochondria significantly contributed to the measured signal, because under our experimental conditions mitochondrial $[Ca^{2+}]$ has been reported to be lower than 100 nM (Andrienko *et al.* 2009).

Measurements of Ca^{2+} blinks

Localized $[Ca^{2+}]_{SR}$ depletions or Ca^{2+} blinks (Brochet *et al.* 2005; Zima *et al.* 2008*b*) and the corresponding local cytosolic Ca^{2+} elevations (Ca^{2+} sparks) were recorded simultaneously with confocal microscopy (Fig. 3*C* and *D*) using Rhod-2 as the cytosolic and Fluo-5N as the SR Ca^{2+} indicator, respectively. For each detected Ca^{2+} spark with Rhod-2, the corresponding local changes of the Fluo-5N signal were analysed. The profiles of Ca^{2+} blinks were fitted with the product of two exponential functions to the declining and recovery phase, respectively, as described previously (Zima *et al.* 2008*b*). Blink amplitudes were obtained from the fit of the experimental data.

Statistics

Data are presented as means ± S.E.M. of n measurements. Statistical comparisons between groups were performed with Student's t test. Differences were considered statistically significant at $P < 0.05$.

Results

The effect of $[Ca^{2+}]_{SR}$ on Ca^{2+} spark properties

To investigate the relationship between Ca^{2+} sparks and SR Ca^{2+} load, we simultaneously measured cytosolic $[Ca^{2+}]$ and $[Ca^{2+}]_{SR}$ in permeabilized ventricular myocytes after complete SERCA inhibition with thapsigargin (TG). Figure 1*A* depicts line-scan images of Rhod-2 and Fluo-5N fluorescence with corresponding profiles of local $[Ca^{2+}]_i$ (including Ca^{2+} sparks) and cell-averaged $[Ca^{2+}]_{SR}$. The recordings were made in control conditions and at different times after application of TG (10 μM). In these experiments, local $[Ca^{2+}]_{SR}$ depletions, Ca^{2+} blinks (Brochet *et al.* 2005; Zima *et al.* 2008*b*), were not resolved because Fluo-5N fluorescence was acquired in non-confocal mode. This strategy allowed us to use very low laser intensity to avoid dye photobleaching and improved the signal-to-noise ratio of Fluo-5N (see Methods). Under control conditions, Ca^{2+} spark frequency and $[Ca^{2+}]_{SR}$ had average values of 10.1 ± 0.8 sparks $(100\ \mu m)^{-1}\ s^{-1}$ and $760 \pm 22\ \mu$M ($n = 16$), respectively. Spark frequency correlated positively with $[Ca^{2+}]_{SR}$ measured under control conditions (no TG present; Fig. 1*B*). After SERCA inhibition, $[Ca^{2+}]_{SR}$ and Ca^{2+} spark frequency gradually declined until sparks ceased completely at $[Ca^{2+}]_{SR} = 279 \pm 10\ \mu$M ($n = 16$ cells) (Fig. 1*C*). After the disappearance of Ca^{2+} sparks, $[Ca^{2+}]_{SR}$ continued to decline until full depletion (verified as lack of response to stimulation with 10 mM caffeine). These results suggest that SR Ca^{2+} leak can occur in form of sparks, but there is also spark-independent leak.

We then analysed how luminal $[Ca^{2+}]$ affects the properties of Ca^{2+} sparks. For each individual cell studied under conditions illustrated in Fig. 1*A*, spark frequency, amplitude, width and duration were plotted as a function of $[Ca^{2+}]_{SR}$. $[Ca^{2+}]_{SR}$ affected spark frequency, amplitude and width in a dose-dependent manner (Fig. 2*A–C*); however, spark duration was not affected (Fig. 2*D*). Ca^{2+} spark frequency was most sensitive to $[Ca^{2+}]_{SR}$. Changes of $[Ca^{2+}]_{SR}$ from 400 to 800 μM increased spark frequency, amplitude and width by 10, 1.8 and 1.6 times, respectively. The relationship between spark frequency and $[Ca^{2+}]_{SR}$ was similar to that previously observed when SERCA was not blocked (Fig. 1*B*), indicating that TG did not directly affect SR Ca^{2+} release. We corrected spark frequency for missing events using a previously tested approach (Song *et al.* 1997). The correction for missing events did not significantly change the relationship between spark frequency and $[Ca^{2+}]_{SR}$ (see Supplemental Material).

These results demonstrate that Ca^{2+} spark frequency, amplitude and width are highly dependent on $[Ca^{2+}]_{SR}$. These might be due to changes of Ca^{2+} release flux as the Ca^{2+} gradient across the SR membrane changes and also could be due to luminal Ca^{2+}-dependent RyR regulation (Sitsapesan & Williams, 1994; Gyorke & Gyorke, 1998).

Contribution of Ca^{2+} sparks to total SR Ca^{2+} leak

Next, we examined to what extent SR Ca^{2+} release through Ca^{2+} sparks contributes to total SR Ca^{2+} leak. Free luminal $[Ca^{2+}]$ after SERCA inhibition was converted to total $[Ca^{2+}]_{SR}$ ($[Ca^{2+}]_{SRT}$) based on the known intra-SR Ca^{2+}-buffer capacity (Shannon *et al.* 2000*b*). SR Ca^{2+} leak rate, which was measured as changes of $[Ca^{2+}]_{SRT}$ over time ($d[Ca^{2+}]_{SRT}/dt$), was plotted against the corresponding free $[Ca^{2+}]_{SR}$ to obtain the relationship between SR Ca^{2+} leak rate and $[Ca^{2+}]_{SR}$ (Fig. 3*A*). We found that the SR Ca^{2+} leak increased as a function of $[Ca^{2+}]_{SR}$, with a particularly steep increase at higher $[Ca^{2+}]_{SR}$ (>600 μM). This increase in the leak rate can be attributed to higher Ca^{2+} spark frequency that occurred at higher $[Ca^{2+}]_{SR}$ (Fig. 2*A*). Higher $[Ca^{2+}]_{SR}$ also led to increased spark amplitude and width (Fig. 2*B* and *C*). Spark signal mass, which is proportional to amplitude and width, has been used previously as a measure of releasable Ca^{2+} during an individual spark (Chandler *et al.* 2003). Therefore, the overall rate of spark-mediated Ca^{2+} leak should be proportional to total spark signal mass. Figure 3*B* shows the relationship between $[Ca^{2+}]_{SR}$ and total spark signal mass. The experimental points were well fitted with a single exponential function with a growth constant of 148 μM (black line). Alternatively, SR Ca^{2+} release flux during a spark can be estimated from the maximum of the first derivative of the cytosolic fluorescence intensity (Sipido & Wier, 1991). The

spark-mediated leak would then be proportional to total spark-mediated release flux. The data were binned and plotted as total spark-mediated release flux *versus* $[Ca^{2+}]_{SR}$ (Fig. 3*B*, red symbols). Similar to the results using the signal mass, the experimental points were well fitted with a single exponential function with a growth constant of 167 μM (red line). These two functions matched well, suggesting that both describe the same process of Ca^{2+} spark-mediated leak. When $[Ca^{2+}]_{SR}$ was depleted below 300 μM, the total spark signal mass and the total spark-mediated release flux became insignificant, indicating the absence of spark-mediated leak. Therefore, at low $[Ca^{2+}]_{SR}$ (<300 μM) SR Ca^{2+} leak occurred mostly as non-spark-mediated leak. The experimental points of SR Ca^{2+} leak at low $[Ca^{2+}]_{SR}$ (between 25 and 325 μM) were best fitted with a Hill function (Fig. 3*A*, green line) with $K_{0.5}$ of 135 μM and V_{max} of 3.9 μM s^{-1}. Next, the spark-mediated leak as a function of $[Ca^{2+}]_{SR}$ was estimated by subtracting the non-spark-mediated leak rate (green line) from the measured total SR Ca^{2+} leak rate (black points). The obtained points could be fitted with a single exponential function with a growth constant of

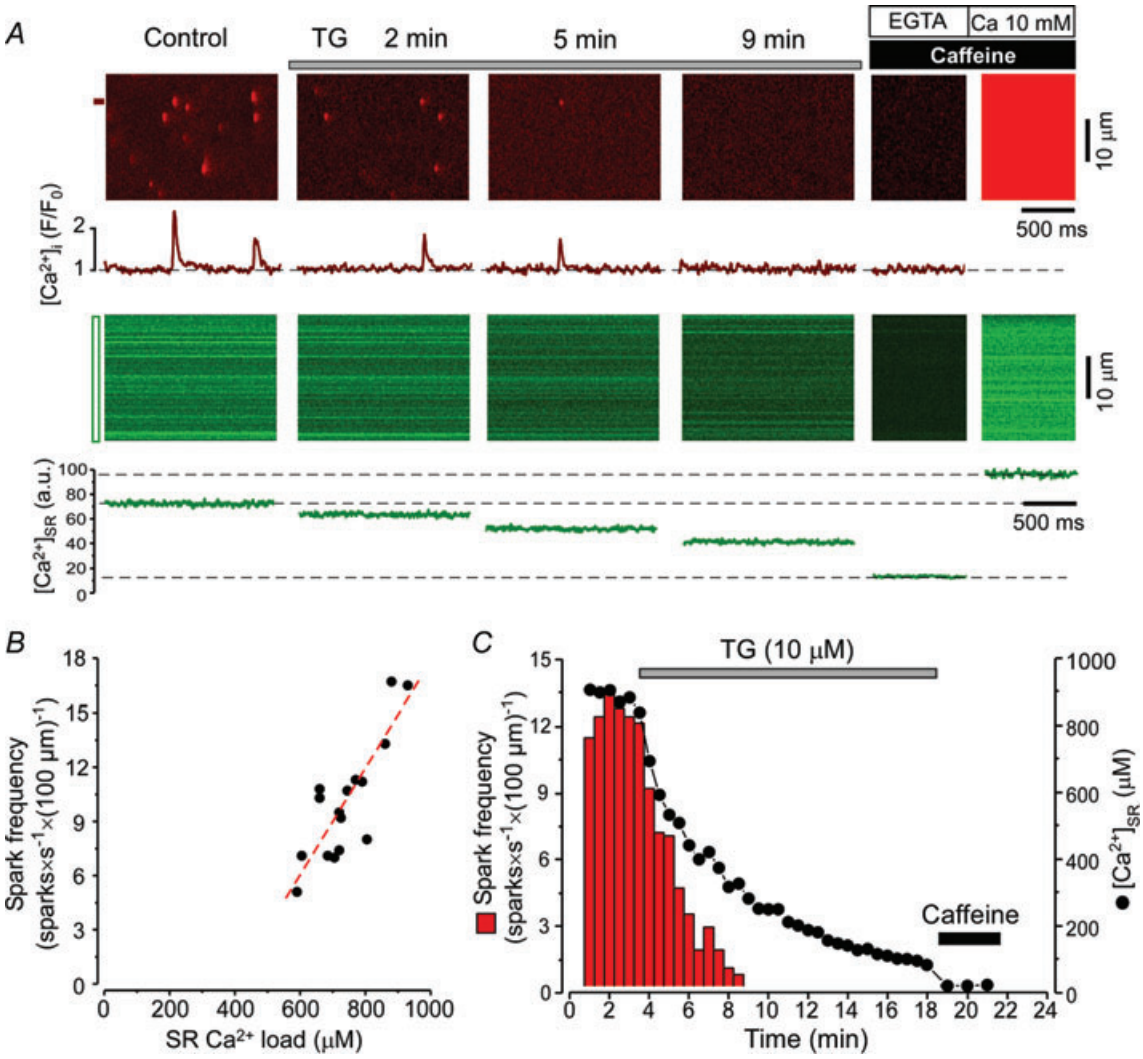

Figure 1. Simultaneous measurements of Ca^{2+} sparks and $[Ca^{2+}]_{SR}$ in permeabilized ventricular myocytes

A, line-scan images and corresponding profiles (F/F_0) of Rhod-2 (red) and Fluo-5N (green) fluorescence in control conditions and at different times after application of thapsigargin (TG; 10 μM). Fluo-5N was recorded with open pinhole (non-confocal setting) whereas Rhod-2 was recorded confocally. The Ca^{2+} spark profiles were obtained by averaging fluorescence from the 1 μm wide region marked by the red box. Fluo-5N profiles were obtained by averaging fluorescence over the entire width of the line-scan images. At the end of the experiment, F_{min} and F_{max} were measured (see Methods). *B*, relationship between initial $[Ca^{2+}]_{SR}$ and Ca^{2+} spark frequency measured under control conditions (before TG application) from 16 different cells. Frequency correlated positively with $[Ca^{2+}]_{SR}$ measured under control conditions ($R^2 = 0.78$). *C*, effects of SERCA inhibition on spark frequency and $[Ca^{2+}]_{SR}$. Measurements were made from the same cell shown in panel *A*.

145 μM (red line), which agrees with the spark-mediated Ca^{2+} leak estimated from the properties of Ca^{2+} sparks (signal mass and release flux) shown in Fig. 3*B*.

In the following experiments, we analysed $[Ca^{2+}]_{SR}$ remaining in the SR at the nadir of Ca^{2+} blinks (Brochet *et al.* 2005; Zima *et al.* 2008*b*). Figure 3*C* shows a representative example of a Ca^{2+} spark and corresponding Ca^{2+} blink simultaneously recorded with confocal microscopy. We have shown previously that Ca^{2+} sparks terminate at an absolute $[Ca^{2+}]_{SR}$ depletion threshold that was independent of SR Ca^{2+} load (Zima *et al.* 2008*b*). Therefore, it is reasonable to predict that Ca^{2+} spark activity, and therefore spark-mediated Ca^{2+} leak, would cease completely at $[Ca^{2+}]_{SR}$ lower than the average spark termination threshold. Fluo-5N signals during Ca^{2+} blinks were converted to $[Ca^{2+}]$ and distribution of $[Ca^{2+}]_{SR}$ at the nadir of blinks was analysed (Fig. 3*D*). On average, Ca^{2+} sparks terminated at 305 ± 11 μM of $[Ca^{2+}]_{SR}$ ($n = 44$ events). This value matched well above estimates of the threshold for spark-mediated Ca^{2+} leak measured from the SR Ca^{2+} leak rate (Fig. 3*A*) and spark properties (Fig. 3*B*).

These results demonstrate that at least two components of SR Ca^{2+} leak can be identified in rabbit ventricular myocytes: Ca^{2+} leak in the form of sparks and non-spark-mediated leak. Depending on $[Ca^{2+}]_{SR}$, these two components contribute to a different degree to the total SR Ca^{2+} leak. At low $[Ca^{2+}]_{SR}$, Ca^{2+} leak occurred mostly as non-spark-mediated leak. At high $[Ca^{2+}]_{SR}$, however, Ca^{2+} sparks became a significant pathway of SR Ca^{2+} leak.

Contribution of RyR-mediated Ca^{2+} leak to total SR Ca^{2+} leak

In the following experiments, we investigated whether spark-independent Ca^{2+} leak still occurred through RyRs. To this end, we studied the effects of the RyR agonist (caffeine) and RyR antagonists (ruthenium red (RuR), Mg^{2+}, or tetracaine) on $[Ca^{2+}]_{SR}$, spark frequency and SR Ca^{2+} leak.

Initially, we studied the effect of a low dose of caffeine, which does not evoke global SR Ca^{2+} release, but substantially sensitizes RyRs. Figure 4*A* shows

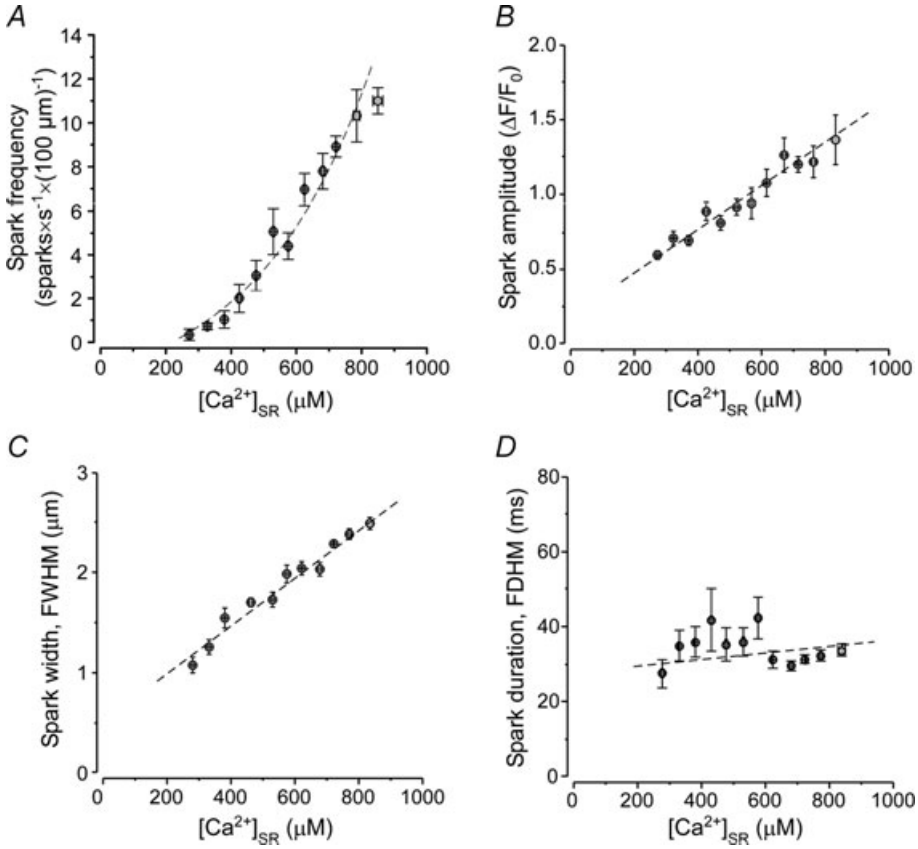

Figure 2. Effect of $[Ca^{2+}]_{SR}$ on Ca^{2+} spark properties
The dependence of spark frequency (*A*), spark amplitude (*B*), spark width (*C*) (measured at half-maximal amplitude, FWHM) and spark duration (*D*) (measured at half-maximal amplitude, FDHM) on $[Ca^{2+}]_{SR}$ (bin size 50 μm; $n = 16$ myocytes).

representative confocal line-scan images of Ca^{2+} sparks and averaged $[Ca^{2+}]_{SR}$ under control conditions, immediately and 2 min after application of caffeine (200 μM), as well as after subsequent addition of TG (10 μM). Caffeine transiently increased Ca^{2+} spark activity and partially depleted the SR (Fig. 4*B*). On average (Fig. 4*C*), spark frequency initially increased from 8.5 ± 0.9 to 14.9 ± 1.2 ($n = 6$; $P < 0.05$), then decreased to 6.1 ± 0.9 sparks $(100\ \mu m)^{-1}\ s^{-1}$ ($n = 6$; $P < 0.05$). After 2 min of caffeine application, $[Ca^{2+}]_{SR}$ decreased from 869 ± 48 to 615 ± 66 μM ($n = 6$; $P < 0.05$; Fig. 4*C*). At the same time when $[Ca^{2+}]_{SR}$ reached a new steady-state level, spark amplitude and width were decreased by 26% ($n = 6$; $P < 0.05$) and by 21% ($n = 6$; $P < 0.05$), respectively. In the presence of caffeine, SERCA inhibition resulted in a faster decline of $[Ca^{2+}]_{SR}$ (by 45%) and Ca^{2+} spark frequency (by 79%) than in the absence of RyR stimulation (Fig. 4*B*). Sparks ceased completely when $[Ca^{2+}]_{SR}$ decreased below 229 ± 32 μM ($n = 6$ cells), which is significantly lower than under control conditions. We measured leak rate as a function of $[Ca^{2+}]_{SR}$ in the presence of caffeine (Fig. 4*D*, red symbols) and compared with the leak rate under control conditions (Fig. 4*D*, black symbols). These data show

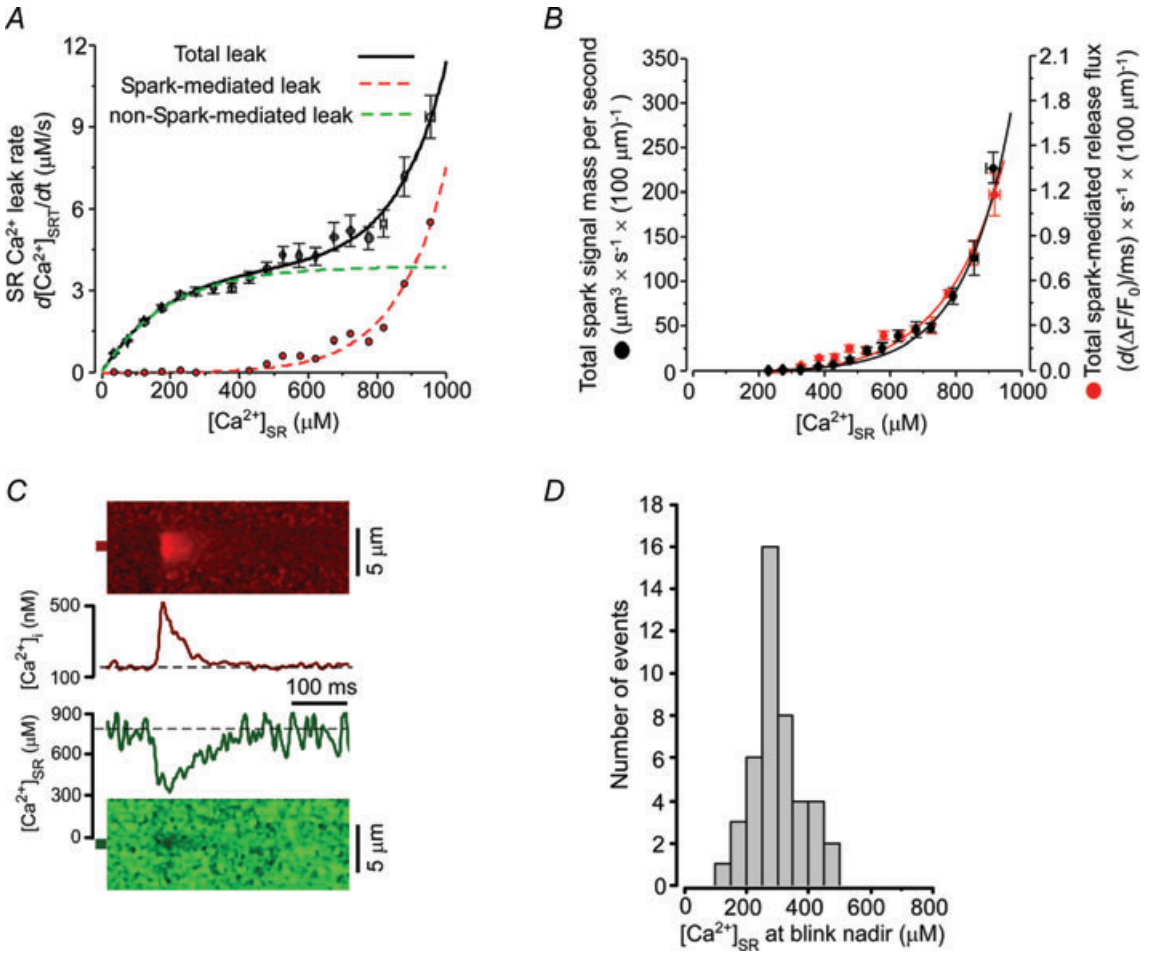

Figure 3. Contribution of Ca^{2+} sparks to total SR Ca^{2+} leak
A, relationships between SR Ca^{2+} leak rate and $[Ca^{2+}]_{SR}$ ($n = 16$ myocytes). Black circles and black line represent experimentally measured total leak. The leak data points between $[Ca^{2+}]_{SR}$ of 25 and 325 μM were fitted with a single sigmoid function and represents the non-spark-mediated leak (green line). Spark-mediated leak as function of $[Ca^{2+}]_{SR}$ was obtained by subtracting non-spark-mediated leak (green line) from total SR Ca^{2+} leak (black circles). The calculated points (red circles) could be fitted with a single exponential function (red line). *B*, dependence of total spark signal mass (black circles) and total spark-mediated Ca^{2+} release flux (red circles) from $[Ca^{2+}]_{SR}$. Signal mass and Ca^{2+} release flux of all detected sparks were summated and normalized to the recording time (4.5 s). Spark signal mass and spark-mediated release flux were calculated as described in Methods. *C*, simultaneously recorded Ca^{2+} spark and blink. Top, line-scan image of Rhod-2 fluorescence and corresponding spark profile (F/F_0). Bottom, line-scan image of Fluo-5N fluorescence and corresponding blink profile. Spark and blink profiles were obtained by averaging fluorescence from the 1 μm the wide regions marked by the red and green box, respectively. *D*, distribution of $[Ca^{2+}]_{SR}$ at the nadir of blinks (44 events).

that sensitization of RyRs with caffeine significantly increased SR Ca^{2+} leak. Therefore, caffeine decreased $[Ca^{2+}]_{SR}$ by stimulation of RyR-mediated Ca^{2+} leak and consequently led to a decrease in SR Ca^{2+} release due to a luminal Ca^{2+}-dependent mechanism (Trafford *et al.* 2000; Lukyanenko *et al.* 2001). Notably at $[Ca^{2+}]_{SR}$ below 170 μM, caffeine did not affect Ca^{2+} leak (Fig. 4*D*). This observation suggests that either caffeine does not activate RyRs at low $[Ca^{2+}]_{SR}$ or that at this $[Ca^{2+}]_{SR}$ Ca^{2+} leak occurs via pathways other than RyRs.

In the next set of experiments, we studied the effects of RyR inhibitors on SR Ca^{2+} leak. We used RuR, Mg^{2+}, or tetracaine at concentrations which completely inhibit RyRs reconstituted in lipid bilayers (Xu *et al.* 1996; Lukyanenko *et al.* 2000; Zima *et al.* 2008*a*) as well as SR Ca^{2+} release in myocytes (Gyorke *et al.* 1997; Lukyanenko *et al.* 2000). RuR (50 μM) completely abolished Ca^{2+} sparks and almost doubled $[Ca^{2+}]_{SR}$, confirming that RyRs provide an important SR Ca^{2+} leak pathway under resting conditions (Fig. 5*A*). Similar results were obtained when RyRs were inhibited with either 15 mM Mg^{2+} (Fig. 5*B*) or 1 mM tetracaine (data not shown). Average results of RyR inhibitors on $[Ca^{2+}]_{SR}$ under control conditions (no TG present) are shown in Fig. 5*C*. Application of TG (10 μM) in the presence of RyR inhibitors resulted in decline of $[Ca^{2+}]_{SR}$, which reached complete depletion within approximately 40 min (Fig. 5*A* and *B*). Compared to control conditions (dashed lines in Fig. 5*A* and *B*), RyR inhibition significantly decreased SR Ca^{2+} leak rate but did not prevent leak. Increasing RuR concentration to 100 μM or combining RuR (50 μM) and Mg^{2+} (15 mM) had no additional effect on Ca^{2+} leak. Figure 5*D* shows effects of RuR (50 μM), Mg^{2+} (15 mM), and tetracaine (1 mM) on SR Ca^{2+} leak over a wide range of $[Ca^{2+}]_{SR}$. For all RyR inhibitors tested here, RuR had the most pronounced effect on SR Ca^{2+} leak. In the presence of RuR, the leak rate was

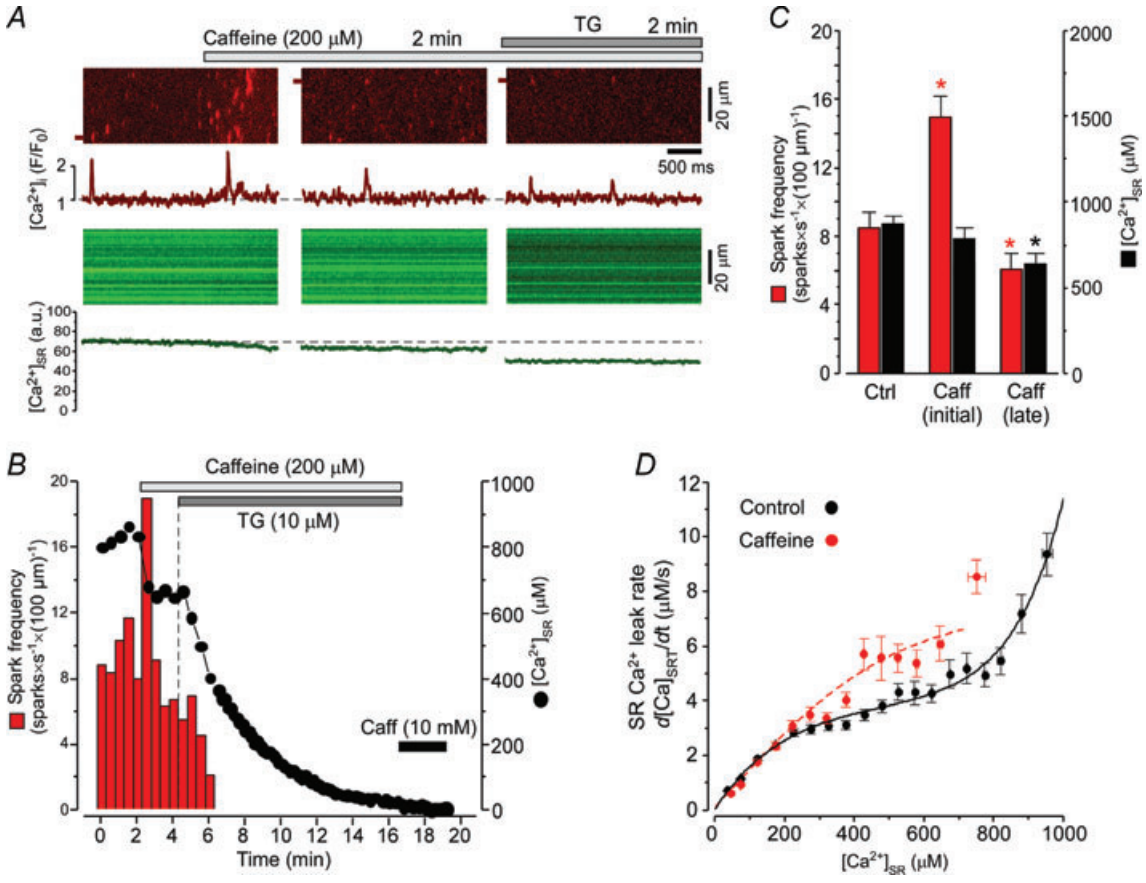

Figure 4. Effects of RyR stimulation by low-dose caffeine on Ca^{2+} sparks, $[Ca^{2+}]_{SR}$ and SR Ca^{2+} leak
A, line-scan images and corresponding profiles of Rhod-2 (red) and Fluo-5N (green) fluorescence in control conditions, in the presence of caffeine (200 μM) and after subsequent application of thapsigargin (TG; 10 μM). Fluo-5N was recorded with open pinhole (non-confocal setting) whereas Rhod-2 was recorded confocally. *B*, effect of caffeine (200 μM) followed by SERCA inhibition (10 μM TG) on spark frequency and $[Ca^{2+}]_{SR}$. Application of 10 mM caffeine at the end of the experiment indicates complete depletion of the SR. Measurements were made from the same cell shown in panel *A*. *C*, average spark frequency and $[Ca^{2+}]_{SR}$ in control conditions, immediately (initial) and 2 min (late) after exposure to caffeine (200 μM). *D*, the relationships between SR Ca^{2+} leak rate and $[Ca^{2+}]_{SR}$ in control conditions (back) and in the presence of caffeine (red).

best fitted with a Hill function with $K_{0.5}$ of 148 μM and V_{max} of 1.5 μM s^{-1}. By subtracting this RuR-insensitive Ca^{2+} leak from the total leak we estimated RyR-mediated Ca^{2+} leak as a function of $[Ca^{2+}]_{SR}$. Figure 6*A* shows different components of SR Ca^{2+} leak in permeabilized rabbit ventricular myocytes.

We also tested whether spontaneous openings of IP_3Rs were responsible for RyR-independent Ca^{2+} leak. The IP_3R inhibitors 2-APB (20 μM; Fig. 6*B*) or heparin (0.5 mg ml^{-1}; not shown) had no additional inhibitory effect on SR Ca^{2+} leak when added together with RuR (50 μM) suggesting that the residual SR Ca^{2+} leak was not the result of IP_3R activity. However, application of IP_3 (20 μM) increased RyR-independent Ca^{2+} leak. At $[Ca^{2+}]_{SR}$ = 780 μM SR Ca^{2+} leak nearly doubled from 1.2 to 2.2 μM s^{-1} (Fig. 6*B*).

These results show that RyRs are the main, but not the sole, contributor to SR Ca^{2+} leak in rabbit ventricular myocytes. Under basal conditions (in the absence of IP_3 production), IP_3R-mediated leak is minimal; however, there is SR Ca^{2+} leak that is RyR and IP_3R independent through a yet to be determined mechanism.

The properties of SR Ca^{2+} leak in ventricular myocytes from failing heart

In the following experiments, we studied properties of SR Ca^{2+} leak in permeabilized ventricular myocytes isolated from failing hearts. Similar to previous studies using the same HF model (Pogwizd *et al.* 2001; Guo *et al.* 2007; Domeier *et al.* 2009), we found that resting $[Ca^{2+}]_{SR}$ was significantly lower in HF myocytes. In normal (nonfailing) myocytes, resting $[Ca^{2+}]_{SR}$ was 760 ± 15 μM (n = 44), whereas under identical experimental conditions $[Ca^{2+}]_{SR}$ was 683 ± 27 μM in HF myocytes (n = 14; $P < 0.05$). Furthermore, the rate of decline of $[Ca^{2+}]_{SR}$ and spark frequency after SERCA inhibition was faster in HF myocytes than in normal myocytes (Fig. 7*A*, compare with

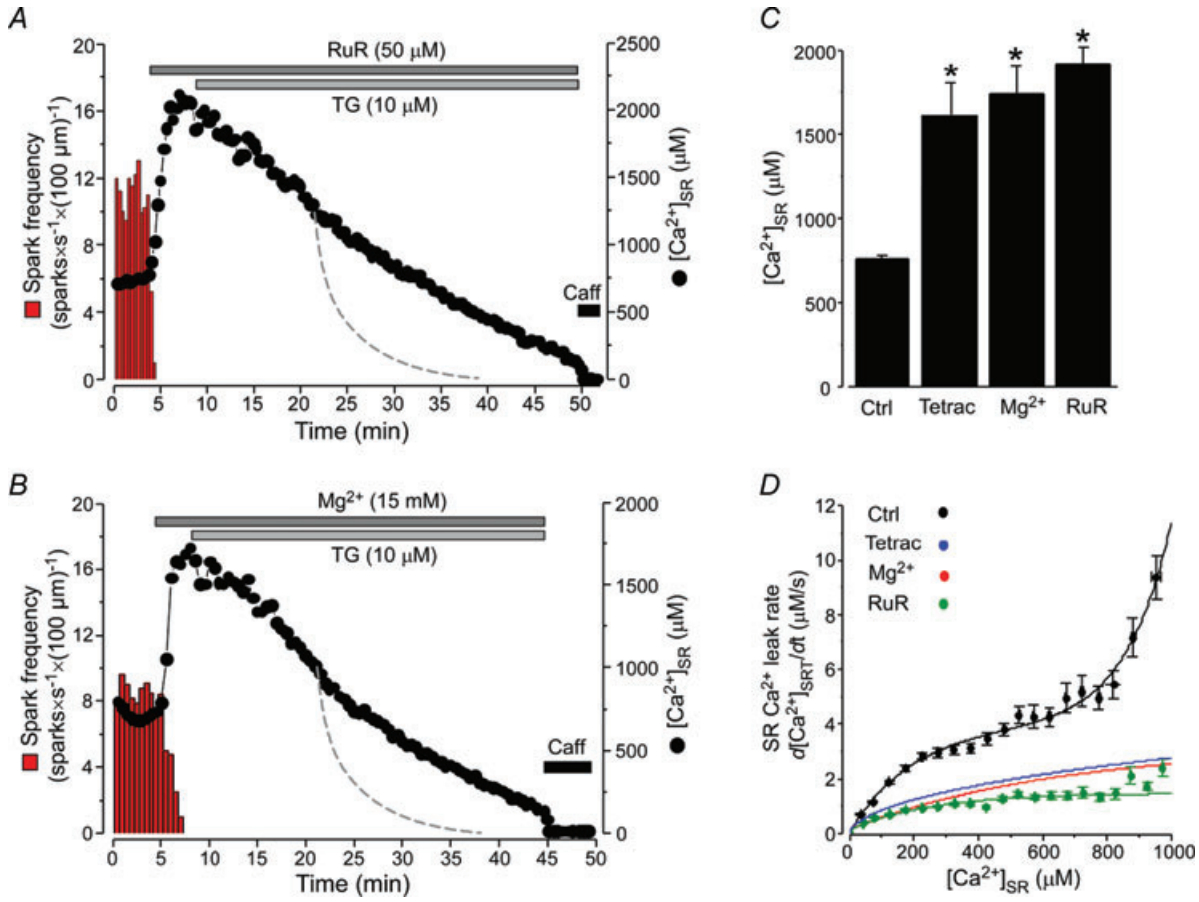

Figure 5. Effects of RyR inhibitors on Ca^{2+} sparks, $[Ca^{2+}]_{SR}$ and SR Ca^{2+} leak
Effect of ruthenium red (RuR; 50 μM) (*A*) and Mg^{2+} (15 mM) (*B*) on spark frequency and $[Ca^{2+}]_{SR}$ before and after SERCA inhibition. For comparison, the dashed lines indicate the decline of $[Ca^{2+}]_{SR}$ in the absence of RyR inhibition (data from Fig. 1*C*). *C*, average effect of RuR (50 μM), Mg^{2+} (15 mM) and tetracaine (1 mM) on $[Ca^{2+}]_{SR}$ in the absence of TG. *D*, the relationships between SR Ca^{2+} leak rate and $[Ca^{2+}]_{SR}$ in control conditions (back), in the presence of RuR (green), tetracaine (blue) and Mg^{2+} (red). For presentation purposes only the fit to the data is shown for tetracaine and Mg^{2+}.

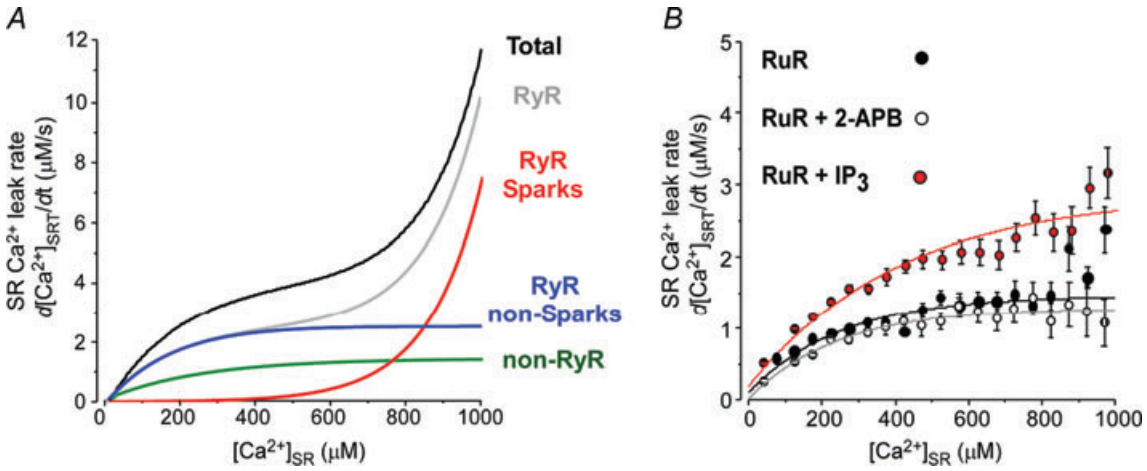

Figure 6. Components of SR Ca^{2+} leak and role of IP_3Rs in SR Ca^{2+} leak
A, different components of SR Ca^{2+} leak rate as a function of $[Ca^{2+}]_{SR}$. Grey line represents the total RyR-mediated Ca^{2+} leak (spark and non-spark). This component was obtained by subtracting RuR-insensitive Ca^{2+} leak (green line) from the total Ca^{2+} leak (black line). Ca^{2+} spark-mediated leak (red line) was obtained as described in Fig. 3*A*. Non-spark RyR-mediated Ca^{2+} leak (blue line) was obtained by subtracting Ca^{2+} spark-mediated leak (red line) from the total RyR-mediated Ca^{2+} leak (grey line). *B*, the relationship between SR Ca^{2+} leak rate and $[Ca^{2+}]_{SR}$ in the presence of RuR (50 μM; black circles), in the presence of RuR plus 2-APB (20 μM; open circles) and in the presence of RuR plus IP_3 (10 μM; red circles).

Fig. 1*C*). The SR Ca^{2+} leak rate was analysed as a function of $[Ca^{2+}]_{SR}$ in HF myocytes (Fig. 7*B*, red symbols) and compared to normal myocytes (Fig. 7*B*, black symbols). We found that at $[Ca^{2+}]_{SR}$ higher than 200 μM Ca^{2+} leak was markedly increased in HF myocytes.

In the presence of RuR (50 μM), SR Ca^{2+} leak was not significantly different between normal and HF myocytes (Fig. 7*B*) suggesting that the increased SR Ca^{2+} leak in HF myocytes was mainly due to higher RyR activity. We then studied if increased SR Ca^{2+} leak in HF myocytes was a result of higher Ca^{2+} spark activity. When Ca^{2+} sparks were analysed for these two groups at the same $[Ca^{2+}]_{SR}$ (680 μM), spark frequency was higher by 21% in HF myocytes (9.3 ± 0.9 sparks $(100\ \mu m)^{-1}\ s^{-1}$; $n = 14$) compared to normal myocytes (7.7 ± 0.8 sparks $(100\ \mu m)^{-1}\ s^{-1}$; $n = 16$; Fig. 7*C*). However, RyR-mediated SR Ca^{2+} leak (estimated as the difference between the total and RuR-insensitive Ca^{2+} leak) measured at the same $[Ca^{2+}]_{SR}$ (680 μM) was significantly higher (by 40%) in HF myocytes (Fig. 7*B*). These results suggest that the modifications of RyRs which occur during HF lead to augmentation of both spark- and non-spark-mediated Ca^{2+} leak.

Discussion

SR Ca^{2+} leak is generally defined as 'basal' Ca^{2+} efflux from the SR during rest or diastole. Despite its low flux

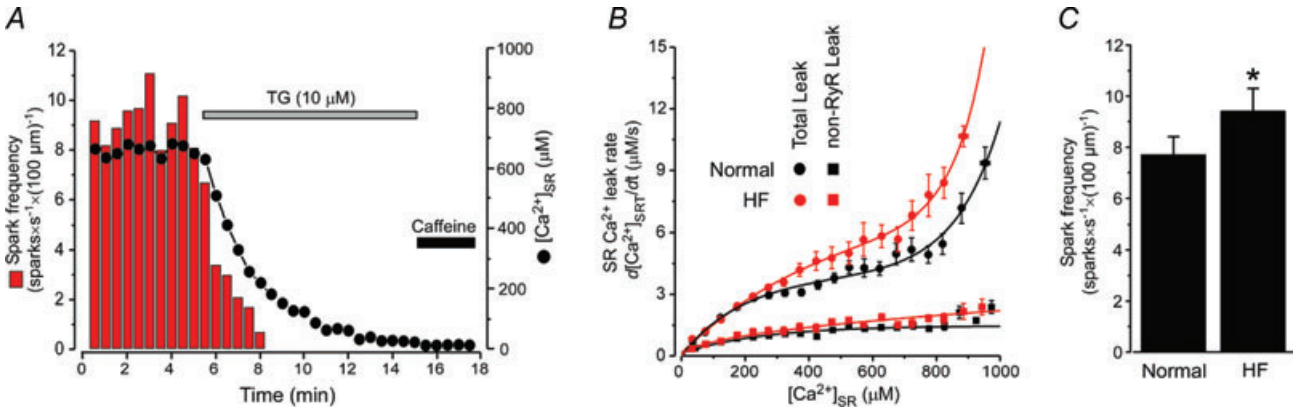

Figure 7. Properties of SR Ca^{2+} leak in HF myocytes
A, changes of spark frequency and $[Ca^{2+}]_{SR}$ after SERCA inhibition with TG (10 μM) in myocyte from failing hearts. *B*, the total (circles) and RuR-insensitive (squares) SR Ca^{2+} leak as a function of $[Ca^{2+}]_{SR}$ in normal (black) and in HF myocytes (red). *C*, Ca^{2+} spark frequency in normal and HF myocytes measured at the same $[Ca^{2+}]_{SR}$ (680 μM).

rate relative to SR Ca^{2+} release during systole, diastolic SR Ca^{2+} leak plays an important role in modulating SR Ca^{2+} load. The RyR is the primary Ca^{2+} release channel of the SR and considered the key pathway of Ca^{2+} leak in ventricular myocytes. Abnormal activity of RyRs has been suggested to be involved in numerous cardiac pathologies, including HF (George, 2008) and catecholaminergic polymorphic ventricular tachycardias (Chelu & Wehrens, 2007). In spite of its importance, the mechanisms of SR Ca^{2+} leak have not been characterized in detail. Here we measure directly and continuously (in real time) SR Ca^{2+} leak properties in normal and HF ventricular myocytes, and determine the role of RyR and Ca^{2+} sparks in SR Ca^{2+} leak. The main findings of this study are that (1) RyR is the key channel of SR Ca^{2+} leak which occurs in part as Ca^{2+} sparks, but there is also spark-independent Ca^{2+} leak; (2) at low $[Ca^{2+}]_{SR}$ leak occurs mostly as non-spark-mediated leak, whereas at high $[Ca^{2+}]_{SR}$ sparks became a significant contributor to SR Ca^{2+} leak; (3) there is also a significant component of SR Ca^{2+} leak that is insensitive to RyR and IP_3R inhibitors (although IP_3R activation can increase leak significantly); and (4) RyR-mediated Ca^{2+} leak is significantly increased in ventricular myocytes from failing heart.

Novel approach to measure SR Ca^{2+} leak

In ventricular myocytes, SR Ca^{2+} leak has been previously measured either from characteristics of Ca^{2+} transients (Balke *et al.* 1994), from the rate of decline in SR Ca^{2+} load after complete SERCA blockade (Bassani & Bers, 1995) or as Ca^{2+} spark properties (Cheng *et al.* 1993). Another method that has been widely used to measure SR Ca^{2+} leak quantifies the decrease of cytosolic $[Ca^{2+}]$ and increase in SR Ca^{2+} content upon acute RyR block with tetracaine (Shannon *et al.* 2002). In the present study, we employed a new approach to measure SR Ca^{2+} leak. We combined direct continuous measurement of $[Ca^{2+}]_{SR}$ using Fluo-5N (Shannon *et al.* 2003*a*; Belevych *et al.* 2007; Domeier *et al.* 2009) with cytosolic Ca^{2+} sparks using Rhod-2 (Brochet *et al.* 2005; Zima *et al.* 2008*b*). This allowed simultaneous measurement of total SR Ca^{2+} leak flux (the rate of $[Ca^{2+}]_{SR}$ decline with SERCA fully blocked) and appearance of Ca^{2+} sparks (one cytosolic readout of SR Ca^{2+} leak).

This approach has several advantages compared to previous studies. First, SR Ca^{2+} leak is measured directly and continuously as changes of $[Ca^{2+}]_{SR}$ after SERCA inhibition with TG. It is essential for the determination of SR Ca^{2+} leak that the SERCA-mediated Ca^{2+} uptake was completely blocked by TG. Here we confirmed that TG (10 μM) completely and irreversibly inhibits SERCA within 1 min (Bassani *et al.* 1995; Zima *et al.* 2008*b*). Second, SR Ca^{2+} leak and $[Ca^{2+}]_{SR}$ can be measured simultaneously over the full physiological range, because $[Ca^{2+}]_{SR}$ gradually declines until full depletion upon SERCA blockade (Fig. 1). Third, using permeabilized myocytes allows cytosolic Fluo-5N washout (providing a more pure $[Ca^{2+}]_{SR}$ signal), cytosolic $[Ca^{2+}]$ can be precisely controlled (so global $[Ca^{2+}]_i$ does not change as $[Ca^{2+}]_{SR}$ declines) and cytosolic Ca^{2+} indicator (Rhod-2) can be introduced to measure cytosolic $[Ca^{2+}]$ and Ca^{2+} sparks. Therefore, in this study for the first time, SR Ca^{2+} load, SR Ca^{2+} leak and Ca^{2+} sparks were measured simultaneously. This is particularly important because Ca^{2+} sparks are often considered to be the main pathway of SR Ca^{2+} leak.

Ca^{2+} sparks are not the sole pathway of SR Ca^{2+} leak

The observation that after SERCA inhibition Ca^{2+} spark frequency declined significantly faster than $[Ca^{2+}]_{SR}$ (Fig. 1*B*) suggests a non-linear relationship between spark frequency and SR Ca^{2+} load. Although it is generally accepted that spark frequency depends on $[Ca^{2+}]_{SR}$ (Satoh *et al.* 1997; Lukyanenko *et al.* 2001), the spark–load relationship had not been rigorously studied because simultaneous measurements of these two characteristics were technically difficult until now. We found that Ca^{2+} spark amplitude and width are linear functions of $[Ca^{2+}]_{SR}$ (Fig. 2*B* and *C*) suggesting that these parameters are mainly determined by the SR to cytosol $[Ca^{2+}]$ gradient. In contrast, Ca^{2+} spark frequency was exponentially dependent on $[Ca^{2+}]_{SR}$ (Fig. 2*A*), suggesting a more complex regulation by $[Ca^{2+}]_{SR}$. Increasing evidence indicates that luminal Ca^{2+} regulates RyR gating by at least two different mechanisms. Ca^{2+} can directly activate RyR from the luminal side of the channel (Sitsapesan & Williams, 1994; Gyorke & Gyorke, 1998), perhaps due to interaction with the Ca^{2+} binding protein calsequestrin (Gyorke *et al.* 2004). Luminal Ca^{2+} can also indirectly regulate RyR by acting on the cytosolic Ca^{2+} activation site of neighbouring channels by a 'feed-through' mechanism (Laver, 2007).

An important finding of this study was that Ca^{2+} sparks entirely disappeared at relatively constant $[Ca^{2+}]_{SR}$ (279 ± 10 μM; Fig. 1). Because Ca^{2+} spark detection relies on their amplitude, the absence of sparks at low $[Ca^{2+}]_{SR}$ might have been the result of a failure to detect Ca^{2+} sparks of smaller amplitudes (i.e. if they fall below the detection threshold). However, we think that is not why Ca^{2+} sparks disappeared at $\sim$300 μM $[Ca^{2+}]_{SR}$, for two major reasons. First, the average spark amplitude at the point of disappearance was $\sim 0.5\ \Delta F/F_0$ (Fig. 2*B*). By analysing the sensitivity of our detection algorithm (see Supplemental Material), we confirmed that at this amplitude the vast majority of sparks ($\sim$70%) are readily detected. Moreover, we have corrected for missed events, and this correction at $0.5\ \Delta F/F_0$ is very small. Second, analysis of $[Ca^{2+}]_{SR}$ at

the nadir of Ca^{2+} blinks (Fig. 3*D*) showed that Ca^{2+} sparks terminate at a relatively constant $[Ca^{2+}]_{SR}$ (305 ± 11 μM), and this termination threshold was independent of SR Ca^{2+} load (Zima *et al.* 2008*b*). Presumably this Ca^{2+} spark termination threshold would also prevent spark initiation (i.e. it would immediately stop). Thus, this disappearance of Ca^{2+} sparks as $[Ca^{2+}]_{SR}$ falls below ~300 μM would be quite consistent with abolition of spark initiation at the same $[Ca^{2+}]_{SR}$ at which Ca^{2+} sparks terminate. If SR Ca^{2+} leak is solely mediated by Ca^{2+} spark activity, then leak should abruptly stop at $[Ca^{2+}]_{SR}$ ~300 μM. However, SR Ca^{2+} leak continued below this $[Ca^{2+}]_{SR}$ suggesting that non-spark mediated Ca^{2+} leak also exists in ventricular myocytes.

SR Ca^{2+} leak can occur as spark-independent RyR openings

We separated SR Ca^{2+} leak into RyR-dependent and RyR-independent components (Fig. 6*A*). The latter is small and persists in the presence of RyR inhibition (Fig. 5); it will be discussed in the next section. The RyR-dependent leak is composed of both a Ca^{2+} spark component (which starts at $[Ca^{2+}]_{SR} \geq 300$ μM and rises steeply at higher $[Ca^{2+}]_{SR}$) and a spark-independent component (apparent at low $[Ca^{2+}]_{SR}$ reaching a plateau at the $[Ca^{2+}]_{SR}$ where Ca^{2+} sparks appear; Fig. 6*A*). The steep $[Ca^{2+}]_{SR}$ dependence of the spark-mediated leak can be explained by the fact that $[Ca^{2+}]_{SR}$ affects both the probability of Ca^{2+} release events (spark frequency) in a non-linear manner (Fig. 2*A*) and the amount of Ca^{2+} released during individual sparks (spark amplitude and width), which increase linearly with $[Ca^{2+}]_{SR}$ (Fig. 2*B* and *C*). Interestingly, the non-spark RyR mediated leak in our analysis is best fitted with a $K_{0.5}$ ~135 μM $[Ca^{2+}]_{SR}$ (Fig. 6*A*), raising the possibility that the same luminal Ca^{2+} site might influence both RyR-dependent pathways (although further tests would be required). The non-spark RyR leak flux seems to be maximal at ~2.5 μM s^{-1}, which is almost 2 times higher than the non-RyR-mediated leak. As $[Ca^{2+}]_{SR}$ rises the Ca^{2+} spark-mediated leak is increasingly dominant (accounting for ~16, 43 and 77% of RyR-mediated leak at 600, 800 and 1000 μM, respectively).

The RyR-mediated leak curve resembles the tetracaine-sensitive SR Ca^{2+} leak reported by Shannon *et al.* (2002) except for two features. First, the spark-independent pedestal component that we see for 100–500 μM $[Ca^{2+}]_{SR}$ was not identified, but they had only one data point for $[Ca^{2+}]_{SR}$ <500 μM. So, this component may have been missed by Shannon *et al.* Second, they found that at $[Ca^{2+}]_{SR} = 1200$ μM leak rose almost vertically and leak reached >21 μmol (litre cytosol)$^{-1}$ s^{-1}. In the present study it was difficult to push $[Ca^{2+}]_{SR}$ that high, in part because some leak occurs as TG block of SERCA is being achieved. If we would extrapolate our curves from Fig. 6*A* up to 1200 μM $[Ca^{2+}]_{SR}$ we may project a similar and very steep leak–load relationship as implied by Shannon *et al.* (2002). This reinforces the notion that there may be a limiting SR Ca^{2+} load due to SR Ca^{2+} leak (Diaz *et al.* 1997), unless leak is blocked by RuR or tetracaine (as in Fig. 5*C*).

So why is some RyR-mediated Ca^{2+} release not spark mediated? The spark-independent RyR leak may still arise from the same RyR clusters responsible for Ca^{2+} spark generation if at low $[Ca^{2+}]_{SR}$ the RyR openings are insufficient to recruit neighbouring RyRs to form a spark. At low $[Ca^{2+}]_{SR}$ RyR openings are briefer (~1/6 as long), carry less current (~1/3 as much), are less sensitive to $[Ca^{2+}]_i$-dependent activation (~10-fold) and have longer latency (~3-fold) (Gyorke & Gyorke, 1998). These aspects could possibly explain the failure of RyR-mediated flux to initiate Ca^{2+} sparks at low $[Ca^{2+}]_{SR}$. At high $[Ca^{2+}]_{SR}$, however, the chance that a single RyR opening can trigger a spark would substantially increase because RyR activation can generate a Ca^{2+} flux large enough to activate the rest of the channels in the cluster. There is also a higher probability that two adjacent channels in the cluster can open simultaneously and increase cytosolic $[Ca^{2+}]$ to the critical level that triggers a spark.

RyR-independent pathways of SR Ca^{2+} leak

Another important finding of this study is that complete block of RyRs did not abolish SR Ca^{2+} leak (Fig. 5). Although the existence of RyR-independent Ca^{2+} leak in ventricular myocytes has been suggested previously, at ~10% of the RyR-mediated Ca^{2+} leak (Neary *et al.* 2002) the mechanisms have not been identified. Our data agree with this and show that the RyR-independent Ca^{2+} leak is a larger fraction of leak at low $[Ca^{2+}]_{SR}$. We tested several potential pathways of RyR-independent Ca^{2+} leak. We have shown previously that IP_3Rs are also expressed in rabbit ventricular myocytes (Wu & Bers, 2006; Domeier *et al.* 2008) and may contribute to this residual SR Ca^{2+} leak. However, IP_3R inhibitors (2-APB and heparin) did not prevent RyR-independent Ca^{2+} leak (Fig. 6*B*) suggesting that IP_3Rs are not contributing to RyR-independent Ca^{2+} leak in our experimental conditions (presumably because IP_3R activation requires IP_3). However, despite low IP_3R expression levels in ventricular myocytes, these channels can participate in diastolic SR Ca^{2+} leak during stimulation of the phospholipase C–IP_3 signalling cascade (e.g. ET-1 receptor activation). In support of this notion, we found that activation of IP_3Rs by IP_3 application nearly doubled RyR-independent SR Ca^{2+} leak (Fig. 6*B*). The 'back-flux' mode of SERCA (Shannon *et al.* 2000*b*) cannot contributes to the RyR-independent Ca^{2+} leak because

all our measurements were carried out with SERCA completely blocked in a dead-end complex by TG. It has been suggested that phospholamban (PLB) pentamers can function as Ca^{2+} channels in lipid bilayers (Kovacs *et al.* 1988). However, Ca^{2+} leak measured from SR vesicles isolated from wild-type and PLB-knockout mouse was not significantly different (Shannon *et al.* 2001). Additionally, it has been shown that the translocon of the rough endoplasmic reticulum is an important Ca^{2+} leak pathway in smooth muscle cells (Amer *et al.* 2009). On the contrary, we did not find any differences in SR Ca^{2+} leak rate when the translocon was opened with puromycin or blocked with anisomycin (data not shown). Therefore, further studies are required to determine the exact molecular mechanisms of RyR-independent SR Ca^{2+} leak and its physiological relevance in cardiomyocytes.

Physiological and pathological significance of SR Ca^{2+} leak

The steep $[Ca^{2+}]_{SR}$ dependence of Ca^{2+} spark dependent leak is paralleled by the efficacy of Ca^{2+}-induced Ca^{2+} release during ECC (Bassani *et al.* 1995; Diaz *et al.* 1997; Shannon *et al.* 2000*a*). For $[Ca^{2+}]_{SR}$ below the threshold for Ca^{2+} spark termination that we report here, L-type Ca^{2+} current cannot induce appreciable SR Ca^{2+} release. Moreover, as $[Ca^{2+}]_{SR}$ increases on the steep part of the Ca^{2+} sparks *vs.* $[Ca^{2+}]_{SR}$ relationship described here, there is an increasingly steep increase in fractional SR Ca^{2+} release for a given Ca^{2+} current. We hypothesize that the same luminal Ca^{2+} sensor increases the probability of spontaneous Ca^{2+} sparks and fractional SR Ca^{2+} release during ECC.

A common characteristic of almost every HF models is a decrease in SR Ca^{2+} content, caused by some combination of decreased SERCA pump function, enhanced Na^+–Ca^{2+} exchange (NCX) function and SR Ca^{2+} leak (George, 2008). Here we eliminated the sarcolemmal Ca^{2+} flux and SERCA effects to directly evaluate SR Ca^{2+} leak in HF myocytes. We found that in HF myocytes SR Ca^{2+} leak for a given $[Ca^{2+}]_{SR}$ was increased to a similar degree as in control cells during exposure to low concentration of caffeine (37 *vs.* 42%, respectively). As a result of this, steady state $[Ca^{2+}]_{SR}$ decreased to a similar level in both groups (683 μM in HF *vs.* 615 μM in the presence of caffeine). Thus, enhanced RyR-mediated leak by itself could largely explain the reduced SR Ca^{2+} load in HF, although functional changes in SERCA, NCX and $[Na^+]_i$ regulation can contribute to the resulting SR Ca^{2+} load in intact HF myocytes (Pogwizd *et al.* 1999; Shannon *et al.* 2003*b*; Despa *et al.* 2002). The increased SR Ca^{2+} leak in HF has been attributed to phosphorylation of the RyR by CaMKII (Ai *et al.* 2005) or protein kinase A (Marx *et al.* 2000) although work in this area is controversial. RyR gating in HF was found to have altered luminal Ca^{2+}-dependent regulation (Kubalova *et al.* 2005), a mechanism that is responsible for Ca^{2+} spark termination (Zima *et al.* 2008*b*) and spark activation (see above). In the same HF model studied here we reported previously that SR Ca^{2+} load is reduced in HF (without altered intra-SR Ca^{2+} buffering), that SR Ca^{2+} release is sensitized to trigger in HF (Guo *et al.* 2007) and that Ca^{2+} sparks terminate at lower $[Ca^{2+}]_{SR}$ (Domeier *et al.* 2009). These may all be interrelated changes in RyR function in HF and this contributes to both altered diastolic and systolic cardiac function in HF.

Conclusion

The fact that RyR inhibition greatly increases SR $[Ca^{2+}]_{SR}$ (Fig. 5*C*) indicates that a significant RyR-mediated Ca^{2+} leak exists under resting conditions and that it limits SR Ca^{2+} load. This implies that at rest SERCA cannot achieve its maximal thermodynamic efficiency and that some ATP is wasted in a futile pump–leak balance. Increased SR Ca^{2+} leak has been implicated in HF and may contribute to triggered arrhythmias (Marx *et al.* 2000; Ai *et al.* 2005). Thus, inhibition of diastolic SR Ca^{2+} release (without inhibiting systolic Ca^{2+} release) would be a potentially important therapeutic strategy. It could have benefits with respect to enhancing energetic efficiency, reducing triggered arrhythmias, limiting myocyte death and limiting the progression from cardiac hypertrophy to HF.

References

Ai X, Curran JW, Shannon TR, Bers DM & Pogwizd SM (2005). Ca^{2+}/calmodulin-dependent protein kinase modulates cardiac ryanodine receptor phosphorylation and sarcoplasmic reticulum Ca^{2+} leak in heart failure. *Circ Res* **97**, 1314–1322.

Amer MS, Li J, O'Regan DJ, Steele DS, Porter KE, Sivaprasadarao A & Beech DJ (2009). Translocon closure to Ca^{2+} leak in proliferating vascular smooth muscle cells. *Am J Physiol Heart Circ Physiol* **296**, H910–H916.

Andrienko TN, Picht E & Bers DM (2009). Mitochondrial free calcium regulation during sarcoplasmic reticulum calcium release in rat cardiac myocytes. *J Mol Cell Cardiol* **46**, 1027–1036.

Balke CW, Egan TM & Wier WG (1994). Processes that remove calcium from the cytoplasm during excitation–contraction coupling in intact rat heart cells. *J Physiol* **474**, 447–462.

Bassani JW, Yuan W & Bers DM (1995). Fractional SR Ca release is regulated by trigger Ca and SR Ca content in cardiac myocytes. *Am J Physiol Cell Physiol* **268**, C1313–C1319.

Bassani RA & Bers DM (1995). Rate of diastolic Ca release from the sarcoplasmic reticulum of intact rabbit and rat ventricular myocytes. *Biophys J* **68**, 2015–2022.

Belevych A, Kubalova Z, Terentyev D, Hamlin RL, Carnes CA & Gyorke S (2007). Enhanced ryanodine receptor-mediated calcium leak determines reduced sarcoplasmic reticulum calcium content in chronic canine heart failure. *Biophys J* **93**, 4083–4092.

Brochet DX, Yang D, Di Maio A, Lederer WJ, Franzini-Armstrong C & Cheng H (2005). Ca^{2+} blinks: rapid nanoscopic store calcium signaling. *Proc Natl Acad Sci U S A* **102**, 3099–3104.

Chandler WK, Hollingworth S & Baylor SM (2003). Simulation of calcium sparks in cut skeletal muscle fibers of the frog. *J Gen Physiol* **121**, 311–324.

Chelu MG & Wehrens XH (2007). Sarcoplasmic reticulum calcium leak and cardiac arrhythmias. *Biochem Soc Trans* **35**, 952–956.

Cheng H, Lederer WJ & Cannell MB (1993). Calcium sparks: elementary events underlying excitation-contraction coupling in heart muscle. *Science* **262**, 740–744.

Despa S, Islam MA, Weber CR, Pogwizd SM & Bers DM (2002). Intracellular Na^+ concentration is elevated in heart failure but Na/K pump function is unchanged. *Circulation* **105**, 2543–2548.

Diaz ME, Trafford AW, O'Neill SC & Eisner DA (1997). Measurement of sarcoplasmic reticulum Ca^{2+} content and sarcolemmal Ca^{2+} fluxes in isolated rat ventricular myocytes during spontaneous Ca^{2+} release. *J Physiol* **501**, 3–16.

Domeier TL, Blatter LA & Zima AV (2009). Alteration of sarcoplasmic reticulum Ca^{2+} release termination by ryanodine receptor sensitization and in heart failure. *J Physiol* **587**, 5197–5209.

Domeier TL, Zima AV, Maxwell JT, Huke S, Mignery GA & Blatter LA (2008). IP_3 receptor-dependent Ca^{2+} release modulates excitation-contraction coupling in rabbit ventricular myocytes. *Am J Physiol Heart Circ Physiol* **294**, H596–H604.

Drummond GB (2009). Reporting ethical matters in *The Journal of Physiology*: standards and advice. *J Physiol* **587**, 713–719.

Franzini-Armstrong C & Protasi F (1997). Ryanodine receptors of striated muscles: a complex channel capable of multiple interactions. *Physiol Rev* **77**, 699–729.

George CH (2008). Sarcoplasmic reticulum Ca^{2+} leak in heart failure: mere observation or functional relevance? *Cardiovasc Res* **77**, 302–314.

Go LO, Moschella MC, Watras J, Handa KK, Fyfe BS & Marks AR (1995). Differential regulation of two types of intracellular calcium release channels during end-stage heart failure. *J Clin Invest* **95**, 888–894.

Guo T, Ai X, Shannon TR, Pogwizd SM & Bers DM (2007). Intra-sarcoplasmic reticulum free $[Ca^{2+}]$ and buffering in arrhythmogenic failing rabbit heart. *Circ Res* **101**, 802–810.

Gyorke I & Gyorke S (1998). Regulation of the cardiac ryanodine receptor channel by luminal Ca^{2+} involves luminal Ca^{2+} sensing sites. *Biophys J* **75**, 2801–2810.

Gyorke I, Hester N, Jones LR & Gyorke S (2004). The role of calsequestrin, triadin, and junctin in conferring cardiac ryanodine receptor responsiveness to luminal calcium. *Biophys J* **86**, 2121–2128.

Gyorke S, Lukyanenko V & Gyorke I (1997). Dual effects of tetracaine on spontaneous calcium release in rat ventricular myocytes. *J Physiol* **500**, 297–309.

Kovacs RJ, Nelson MT, Simmerman HK & Jones LR (1988). Phospholamban forms Ca^{2+}-selective channels in lipid bilayers. *J Biol Chem* **263**, 18364–18368.

Kubalova Z, Terentyev D, Viatchenko-Karpinski S, Nishijima Y, Gyorke I, Terentyeva R, da Cunha DN, Sridhar A, Feldman DS, Hamlin RL, Carnes CA & Gyorke S (2005). Abnormal intrastore calcium signaling in chronic heart failure. *Proc Natl Acad Sci U S A* **102**, 14104–14109.

Laver DR (2007). Ca^{2+} stores regulate ryanodine receptor Ca^{2+} release channels via luminal and cytosolic Ca^{2+} sites. *Biophys J* **92**, 3541–3555.

Lipp P & Niggli E (1996). Submicroscopic calcium signals as fundamental events of excitation–contraction coupling in guinea-pig cardiac myocytes. *J Physiol* **492**, 31–38.

Lukyanenko V, Gyorke I, Subramanian S, Smirnov A, Wiesner TF & Gyorke S (2000). Inhibition of Ca^{2+} sparks by ruthenium red in permeabilized rat ventricular myocytes. *Biophys J* **79**, 1273–1284.

Lukyanenko V, Viatchenko-Karpinski S, Smirnov A, Wiesner TF & Gyorke S (2001). Dynamic regulation of sarcoplasmic reticulum Ca^{2+} content and release by luminal Ca^{2+}-sensitive leak in rat ventricular myocytes. *Biophys J* **81**, 785–798.

Marx SO, Reiken S, Hisamatsu Y, Jayaraman T, Burkhoff D, Rosemblit N & Marks AR (2000). PKA phosphorylation dissociates FKBP12.6 from the calcium release channel (ryanodine receptor): defective regulation in failing hearts. *Cell* **101**, 365–376.

Neary P, Duncan AM, Cobbe SM & Smith GL (2002). Assessment of sarcoplasmic reticulum Ca^{2+} flux pathways in cardiomyocytes from rabbits with infarct-induced left-ventricular dysfunction. *Pflugers Arch* **444**, 360–371.

Picht E, Zima AV, Blatter LA & Bers DM (2007). SparkMaster: Automated calcium spark analysis with ImageJ. *Am J Physiol Cell Physiol* **293**, C1073–1081.

Pogwizd SM (1995). Nonreentrant mechanisms underlying spontaneous ventricular arrhythmias in a model of nonischemic heart failure in rabbits. *Circulation* **92**, 1034–1048.

Pogwizd SM, Qi M, Yuan W, Samarel AM & Bers DM (1999). Upregulation of Na^+/Ca^{2+} exchanger expression and function in an arrhythmogenic rabbit model of heart failure. *Circ Res* **85**, 1009–1019.

Pogwizd SM, Schlotthauer K, Li L, Yuan W & Bers DM (2001). Arrhythmogenesis and contractile dysfunction in heart failure: Roles of sodium-calcium exchange, inward rectifier potassium current, and residual β-adrenergic responsiveness. *Circ Res* **88**, 1159–1167.

Proven A, Roderick HL, Conway SJ, Berridge MJ, Horton JK, Capper SJ & Bootman MD (2006). Inositol 1,4,5-trisphosphate supports the arrhythmogenic action of endothelin-1 on ventricular cardiac myocytes. *J Cell Sci* **119**, 3363–3375.

Santiago DJ, Curran JW, Bers DM, Lederer WJ, Stern MD, Rios E & Shannon TR (2010). Ca sparks do not explain all ryanodine receptor-mediated SR Ca leak in mouse ventricular myocytes. *Biophys J* **98**, 2111–2120.

Satoh H, Blatter LA & Bers DM (1997). Effects of $[Ca^{2+}]_i$, SR Ca^{2+} load, and rest on Ca^{2+} spark frequency in ventricular myocytes. *Am J Physiol Heart Circ Physiol* **272**, H657–H668.

Shannon TR, Chu G, Kranias EG & Bers DM (2001). Phospholamban decreases the energetic efficiency of the sarcoplasmic reticulum Ca pump. *J Biol Chem* **276**, 7195–7201.

Shannon TR, Ginsburg KS & Bers DM (2000*a*). Potentiation of fractional sarcoplasmic reticulum calcium release by total and free intra-sarcoplasmic reticulum calcium concentration. *Biophys J* **78**, 334–343.

Shannon TR, Ginsburg KS & Bers DM (2000*b*). Reverse mode of the sarcoplasmic reticulum calcium pump and load-dependent cytosolic calcium decline in voltage-clamped cardiac ventricular myocytes. *Biophys J* **78**, 322–333.

Shannon TR, Ginsburg KS & Bers DM (2002). Quantitative assessment of the SR Ca^{2+} leak-load relationship. *Circ Res* **91**, 594–600.

Shannon TR, Guo T & Bers DM (2003*a*). Ca^{2+} scraps: local depletions of free $[Ca^{2+}]$ in cardiac sarcoplasmic reticulum during contractions leave substantial Ca^{2+} reserve. *Circ Res* **93**, 40–45.

Shannon TR, Pogwizd SM & Bers DM (2003*b*). Elevated sarcoplasmic reticulum Ca^{2+} leak in intact ventricular myocytes from rabbits in heart failure. *Circ Res* **93**, 592–594.

Sipido KR & Wier WG (1991). Flux of Ca^{2+} across the sarcoplasmic reticulum of guinea-pig cardiac cells during excitation–contraction coupling. *J Physiol* **435**, 605–630.

Sitsapesan R & Williams AJ (1994). Regulation of the gating of the sheep cardiac sarcoplasmic reticulum Ca^{2+}-release channel by luminal Ca^{2+}. *J Membr Biol* **137**, 215–226.

Sobie EA, Guatimosim S, Gomez-Viquez L, Song LS, Hartmann H, Saleet JM & Lederer WJ (2006). The Ca^{2+} leak paradox and rogue ryanodine receptors: SR Ca^{2+} efflux theory and practice. *Prog Biophys Mol Biol* **90**, 172–185.

Song LS, Stern MD, Lakatta EG & Cheng H (1997). Partial depletion of sarcoplasmic reticulum calcium does not prevent calcium sparks in rat ventricular myocytes. *J Physiol* **505**, 665–675.

Terentyev D, Gyorke I, Belevych AE, Terentyeva R, Sridhar A, Nishijima Y, de Blanco EC, Khanna S, Sen CK, Cardounel AJ, Carnes CA & Gyorke S (2008). Redox modification of ryanodine receptors contributes to sarcoplasmic reticulum Ca^{2+} leak in chronic heart failure. *Circ Res* **103**, 1466–1472.

Trafford AW, Sibbring GC, Diaz ME & Eisner DA (2000). The effects of low concentrations of caffeine on spontaneous Ca release in isolated rat ventricular myocytes. *Cell Calcium* **28**, 269–276.

Wu X & Bers DM (2006). Sarcoplasmic reticulum and nuclear envelope are one highly interconnected Ca^{2+} store throughout cardiac myocyte. *Circ Res* **99**, 283–291.

Xu L, Mann G & Meissner G (1996). Regulation of cardiac Ca^{2+} release channel (ryanodine receptor) by Ca^{2+}, H^+, Mg^{2+}, and adenine nucleotides under normal and simulated ischemic conditions. *Circ Res* **79**, 1100–1109.

Zima AV & Blatter LA (2009). Properties of sarcoplasmic reticulum Ca leak in rabbit ventricular and atrial myocytes. *Biophys J* **96**, 276a–277a.

Zima AV, Picht E, Bers DM & Blatter LA (2008*a*). Partial inhibition of sarcoplasmic reticulum Ca release evokes long-lasting Ca release events in ventricular myocytes: role of luminal ca in termination of Ca release. *Biophys J* **94**, 1867–1879.

Zima AV, Picht E, Bers DM & Blatter LA (2008*b*). Termination of cardiac Ca^{2+} sparks: role of intra-SR $[Ca^{2+}]$, release flux, and intra-SR Ca^{2+} diffusion. *Circ Res* **103**, e105–e115.

Author contributions

A.V.Z., E.B., L.A.B. and D.M.B. contributed to the conception and design of the study, interpretation of data and writing of the manuscript. A.V.Z. and E.B. performed the experimental work and analysis of results. All authors have approved the version to be published. All experiments were carried out at Loyola University Chicago and Rush University Medical Center, Chicago.

Acknowledgements

This work was supported by National Institutes of Health Grants HL62231 (L.A.B.) and HL80101 (D.M.B., L.A.B.). The authors also would like to thank Drs Steven Pogwizd for providing rabbit heart failure myocytes, E. Picht for help in approach development and T. L. Domeier and J. T. Maxwell for critical reading of the manuscript.